sciendo

LATVIAN JOURNAL OF PHYSICS
AND TECHNICAL SCIENCES
2024, N 3

DOI: 10.2478/lpts-2024-0021

RECONSTRUCTION OF ELECTROPHYSICAL PARAMETER DISTRIBUTION DURING EDDY CURRENT MEASUREMENTS OF STRUCTURAL FEATURES OF PLANAR METAL OBJECTS

V. Ya. Halchenko, R. Trembovetska, V. Tychkov*, N. Tychkova

Instrumentation,
Mechatronics and Computer Technologies Department
Cherkasy State Technological University,
Blvd. Shevchenka, 460, 18006, Cherkasy, Ukraine
*e-mail: v.tychkov@chdtu.edu.ua

The paper proposes a method of simultaneous reconstruction of the electrical conductivity and magnetic permeability profiles of planar metal research objects based on the results of single measurements by eddy current probes using surrogate optimization techniques in a reduced compact subspace design and accumulating the full amount of the most important a priori information about the modes of electromagnetic objects. In addition to the information on the response of probe signals to changes in electrophysical parameters, a priori information includes the data on multifrequency sensing and changes in the lift-off between metal research objects and eddy current probes. All the main stages for the implementation of the method of solving the inverse problem are demonstrated, namely, creating a uniform computer quasi-design of the experiment with improved 2D-projections based on LP-Sobol's sequences; creating surrogate models on fully connected deep neural networks; reducing the dimensionality of the full design space using the principal components method of PCA; reconstructing profiles as a result of surrogate optimisation in a compact subspace. Numerical examples of the method are also presented in the paper.

Keywords: *compact design subspace, eddy current measurements, planar metal research object, profiles of electrophysical parameters, surrogate optimisation.*

1. INTRODUCTION

As a result of various physical factors acting on metal research objects (MRO), such as temperature, deformation, chemical, and other influences, a certain modification of the properties of their sub-surface zone is observed due to changes in the microstructure. This effect is widely used in engineering applications, such as diagnosing critical conditions of industrial equipment, technological operations for strengthening the surface of metal products, etc. Determination of the electrical conductivity (EC) and magnetic permeability (MP) distributions, which are structure-sensitive electrophysical parameters, at a shallow depth from the surface of metal products, i.e., EC and MP profiles, allows tracking the changes in the mechanical properties of the MROs on the basis of appropriate correlations. It is advisable to use non-destructive testing methods for this purpose, namely, the eddy current method. The method is based on the process of the electromagnetic excitation field interaction with the controlled MRO when it penetrates into the depth and the subsequent registration of the total field due to the result of the mutual influence of the secondary field generated by eddy currents in the MRO and the primary field in the form of the induced EMF in the pick-up coil of the surface transformer probe. Thus, the simultaneous reconstruction of the electrophysical parameter profiles based on eddy current measurements is an urgent problem that can be classified as an inverse problem and whose solution is of scientific interest with a given accuracy.

Parametric nonlinear optimisation, which consists in reconstruction of the EC and MP distributions by minimising the discrepancies in a least-squared sense between the measured values of the probe EMF and the calculated theoretical values obtained by solving the direct problem, is the most common approach to solving the issue. The computational process depends on the complexity of the target function, since it requires a significant number of iterations of the direct solver. It becomes a substantial problem with a "heavy" computationally intensive forward direct model.

Methods of local, in particular the ones with gradients for extremum search, and global optimisation [1], [2], were used in the problems with the electrophysical parameter profiles. Their thorough review is given in [3]. Some applications of local optimisation methods are reported in [4], the peculiarity of which is the use of forward and adjoint methods to calculate the Jacobian matrix. To improve the search capabilities of local optimization methods, various modifications are used, for example, in [5], the Newton-Raphson method with regularization and the use of an unmodified sensitivity matrix is proposed to solve ill-posed and ill-conditioning problems, which makes it possible to eliminate the ill-conditioning of computation during the process of reconstruction and to meet the requirements for calculation accuracy.

However, the use of global extremum search methods [6], which find the minimum of a multimodal target function of complex topography in hyperspace in a small number of iterations without strict requirements for the points of initial approximation, proves to be more promising for this purpose. The most famous representative of this class of algorithms is the bioinspired stochastic evolutionary genetic GA. A significant number of algorithms of this class based on metaheuristics are also widely used in practice.

Surrogate optimisation is used for

cases of time-consuming target functions of optimisation algorithms, which are typical for the tasks of determining the EC and MP profiles, which consists in replacing of "heavy" functions with their high-performance alternatives, namely surrogate models (meta-models) [7].

However, due to the "curse of dimensionality", the problem becomes more critical as the dimensionality of the design space increases, which is also true for profile reconstruction tasks. The large dimensionality of the space requires the creation of cumbersome meta-models and, as a result, large training samples. Reducing the requirements for the volume and quality of training samples is an effective and promising way to improve surrogate optimisation, since the number of points in the training set for creating a meta-model required to correctly sample the design space increases exponentially with the growth of its dimensionality. In addition, a significant number of variables in the optimization algorithm negatively affects the accuracy of the extremum search. Therefore, it makes sense to improve approaches to determining the EC and MP distributions based on modern efficient optimisation techniques, which allows solving both the problems of using resource-intensive for calculating the target functions and reducing the number of variables in search algorithms, and, accordingly, improving the accuracy of solving extreme problems.

2. RESEARCH METHODOLOGY

The task of reconstructing the EC and MP profiles in the optimisation formulation is to minimise the following target function:

$$F(\sigma,\mu,f,z) = \left(C_{mes} - G_{mod}\right)^2 + \left(D_{mes} - Z_{mod}\right)^2 \rightarrow min, \quad (1)$$

where $e_{mes} = C_{mes} + j \cdot D_{mes}$ is the value of the EMF measured by the eddy current probe (ECP) in the algebraic form of writing a complex number with real C_{mes} and imaginary D_{mes} as its parts; $e_{mod} = G_{mod} + j \cdot Z_{mod}$ is the theoretical value of the EMF calculated in accordance with the electrodynamic model, which is a mathematical formulation of the direct problem; σ, μ are the corresponding vectors of electrophysical parameters that determine the desired profiles; f is the frequency of the electromagnetic field excitation; z is the lift-off between the eddy current probe and the surface of the MRO.

The determination of the electrophysical parameter profiles involves the consideration and use of the forward and inverse problems in combination. The Uzal-Cheng-Dodd-Deeds electrodynamic model [8]–[11] of the direct problem in the analytical form used in this research was created under the following assumptions: MROs are characterised by infinite overall dimensions, the medium is assumed to be linear, homogeneous, and isotropic; the electromagnetic field is excited by an ECP generator coil with a sinusoidal current I varying with an angular frequency $\omega = 2 \cdot \pi \cdot f$; the ECP excitation coil has a rectangular cross-section with finite dimensions, is characterised by a uniform current density across the cross-section i_0 and the number of turns W; the measuring coil has a number of turns w_{mes} and an infinite small cross-section. Usually,

the sub-surface zone of the MRO to simulate the continuity of the electrophysical parameter profiles is assumed to be conditionally multilayer. Each layer out of L possible is characterised by constant EC and MP parameters, i.e., a piecewise constant approximation of the profiles occurs. The model, due to its matrix representation, allows for the introduction of an arbitrary number of conditional discretization layers for calculations, which makes it versatile and rather convenient for numerical experiments. It appears to be essential for achieving acceptable modeling accuracy. It should be noted that the existing experience of its use by researchers indicates the necessity to discretize the sub-surface zone into several hundred conditional layers. The model piecewise constant representation of the profiles provides the ability to set any law of the EC and MP distribution, which allows the chosen model to consider various variants of measurement cases. In the future, the electrodynamic model will be used in the modified form proposed by Theodoulidis [12] and presented below:

$$e_{\text{mod}} = -j \cdot \omega \cdot w_{mes} \cdot \oint_{Lc} A(P) dl_p , \tag{2}$$

where:

$$A(r_\delta, z_\delta) = \int_0^\infty J_1(\kappa r_\delta) \cdot [C_s \cdot e^{\kappa z_\delta} + D_{ec} \cdot e^{-\kappa z_\delta}] d\kappa;$$

$$C_s = \frac{\mu_0 \cdot i_0}{2} \cdot \frac{\chi(\kappa r_1, \kappa r_2)}{\kappa^3} \cdot (e^{-\kappa z_1} - e^{-\kappa z_2});$$

$$D_{ec} = \frac{(\kappa \cdot \mu_{t+1} - \lambda_1) \cdot V_{11}(1) + (\kappa \cdot \mu_{t+1} + \lambda_1) \cdot V_{21}(1)}{(\kappa \cdot \mu_{t+1} + \lambda_1) \cdot V_{11}(1) + (\kappa \cdot \mu_{t+1} - \lambda_1) \cdot V_{21}(1)} \cdot C_s;$$

$$i_0 = W \cdot I(r_2 - r_1)^{-1} \cdot (z_2 - z_1)^{-1};$$

$$\chi(x_1, x_2) = \left\{ x_1 \cdot J_0(x_1) - 2 \cdot \sum_{m=0}^{\infty} J_{2m+1}(x_1) \right\} - \left\{ x_2 \cdot J_0(x_2) - 2 \cdot \sum_{m=0}^{\infty} J_{2m+1}(x_2) \right\};$$

$$V(1) = T(1,2) \cdot T(2,3) \cdots T(L-2, L-1) \cdot T(L-1, L);$$

$$T_{11}(t, t+1) = \frac{1}{2} \cdot e^{(-\lambda_{t+1} + \lambda_t) dt} \cdot \left(1 + \frac{\mu_t}{\mu_{t+1}} \cdot \frac{\lambda_{t+1}}{\lambda_t} \right);$$

$$T_{12}(t, t+1) = \frac{1}{2} \cdot e^{(\lambda_{t+1} + \lambda_t) dt} \cdot \left(1 - \frac{\mu_t}{\mu_{t+1}} \cdot \frac{\lambda_{t+1}}{\lambda_t} \right);$$

$$T_{21}(t, t+1) = \frac{1}{2} \cdot e^{(-\lambda_{t+1} - \lambda_t) dt} \cdot \left(1 - \frac{\mu_t}{\mu_{t+1}} \cdot \frac{\lambda_{t+1}}{\lambda_t} \right);$$

$$T_{22}(t, t+1) = \frac{1}{2} \cdot e^{(\lambda_{t+1} - \lambda_t) dt} \cdot \left(1 + \frac{\mu_t}{\mu_{t+1}} \cdot \frac{\lambda_{t+1}}{\lambda_t} \right);$$

$$\lambda_t = \left(\kappa^2 + j \cdot \omega \cdot \mu_0 \cdot \mu_t \cdot \sigma_t \right)^{1/2};$$

$A(r_\delta, z_\delta)$ is the azimuthal component of the vector potential, Wb/m; **V**(1) is a matrix containing elements V_{11}, V_{21}; **T**() is a matrix with elements $T_{11}()$, $T_{12}()$, $T_{21}()$, $T_{22}()$; $\mu_0 = 4\cdot\pi\cdot10^{-7}$ is the magnetic constant, H/m; μ_t is the relative magnetic permeability of the conditional layer t; $J_0()$, $J_1()$, $J_m()$ are cylindrical Bessel functions of the first kind of zero, first, and m orders; r_δ, z_δ are the coordinates of the observation point P in the cylindrical coordinate system, m; $(r_2–r_1)$ is the width of the cross-section of the ECP excitation coil, m; $(z_2–z_1)$ is the height of the cross-section of the ECP excitation coil, m; Lc is the contour of the ECP measuring coil.

The authors created a program code that implements the electrodynamic model in the MathCAD 15 environment. It was verified by numerical calculations by the finite element method for a three-layer MRO in the COMSOL Multiphysics environment using the AC/DC Module [13]. The maximum relative error in determining the vector potential was no more than 0.2 % in amplitude and 0.5 % in phase. Also, additional testing was performed by comparing with the calculations based on analytical models obtained for one- and two-layer MROs [14], which demonstrated significantly higher accuracy rates. Finally, we tested the experimental data presented in [15] for the magnetic induction vector in the centre and below the ECP excitation coil obtained by A. Philippe [16] and K. Kawashima [17], which proved the adequacy of the solution of the direct problem by the created software.

Using the electrodynamic model (2), the theoretical values of the ECP EMF are calculated, which are used in the target function (1). However, it leads to significant problems in the operation of the optimization algorithm due to the significant time spent on even once calculating e_{mod} values. Therefore, in accordance with the idea of surrogate modelling, this model needs to be replaced by a computationally efficient alternative, namely, a meta-model that approximates the "exact" electrodynamic model with high accuracy. That is, formula (1) is transformed to form (3):

$$F\left(\boldsymbol{\sigma},\boldsymbol{\mu},f,z\right) = \left(C_{mes} - G_{metamod}\right)^2 + \left(D_{mes} - Z_{metamod}\right)^2 \rightarrow min, \quad (3)$$

where $e_{metamod} = G_{metamod} + j\cdot Z_{metamod}$ is the theoretical value of the EMF calculated using a neural network proxy-model (meta-model) for the electrodynamic model.

A deep fully connected neural network (DFCNN) serves as an approximator in these studies, which, due to its outstanding generalization capability, is a modern universal tool for performing the relevant tasks. In addition to its high computational performance, the meta-model serves as a storage device for information about the MRO obtained by preliminary modelling in accordance with the created design of experiment (DOE) in various modes of eddy current measurements. An essential feature of this research is that the meta-model takes into account all the factors that mostly affect the formation of the ECP output signal. These undoubtedly include the vectors σ and μ of the electrophysical parameters, and additional factors, in particular, the frequency of the electromagnetic excitation field frequency f and the lift-off z between the ECP and the MRO surface. Since the ECP output signal is characterised by certain values of amplitude and phase in the exponential form, it is necessary to use a complex-valued neural network, whose inputs are real numbers and whose output is complex. For simplicity, it is advisable to replace the complex-valued neural network

by splitting it into two real-valued ones with common inputs. It is useful to consider the outputs of each of the two networks as the real and imaginary parts of the EMF of the ECP, respectively, which eliminates the inconvenience of working with relatively small phase values. Given the complex and significantly nonlinear nature of dependence (2), it is justified to use deep learning for neural networks.

Obtaining an accurate meta-model largely depends on the size and quality of the training sample. These requirements can be met if a perfect DOE is used to create it. To effectively implement the profile reconstruction method, the authors created advanced computer uniform DOEs on quasi-Sobol's sequences [18]. Low discrepancy is their advantage over known designs [19]–[21], and most importantly, in two-dimensional projections. It is these properties of the designs that ensure the accuracy of approximation of complex response hypersurfaces in cases where nothing is known a priori about their topographic features. One of the variants of such quasi-DOEs was used in this research.

The minimisation of the target function (3) was performed by a hybrid multi-agent particle swarm optimisation algorithm with evolutionary formation of the swarm composition [22]–[25] with improved search capabilities. It is a global extremum search algorithm which is of stochastic nature and based on metaheuristics. Due to its stochasticity, a series of algorithm runs were performed to improve the accuracy of the calculations, followed by averaging the results, i.e., the multi-start technique was used. However, the search for an extremum was not carried out in the full design hyperspace, but in its compact subspace, which is characterised by a smaller dimensionality while retaining almost all the properties of the full one without critical loss of information. Finding an extremum in the reduced dimension space makes it possible to take full advantage of the benefits of this approach, described earlier in the introduction. The transition from a multidimensional space to a low-dimensional space was performed using the principal component analysis (PCA) [26]. This is a classical statistical method designed to detect the so-called active new orthogonal basis in the full multidimensional space [27]–[29] based on linear transformations. The basis vectors were found by analysing the singular numbers obtained by the SVD decomposition of the Gram matrix, determined for the data of the full design space. The larger the singular number, the more information is contained in the corresponding eigenvector of the Gram matrix, which is included as a component of the new basis. In this case, the components of the basis maximally preserving information about the MRO were chosen. It allows controlling the choice of the dimension of the compact subspace by mens of balancing. The data concentrated in the full space were projected into the new basis, preserving the essential properties of their originals with the minimal loss. An important advantage of PCA is the ability to back-project the solution data into the original full space after optimisation in the reduced subspace, where the electrophysical parameters of distribution are obtained. It should also be noted that the creation of the meta-model in this case is carried out in a compact subspace, which has a positive effect on the cumbersomeness of its structure, i.e., reducing the number of neurons in the input and hidden layers, etc. In addition, the optimization algorithm operates with normalized values, as this condition is mandatory for neural networks. All these factors together contribute to a higher accuracy of the solution.

It should also be noted that to verify

the solution of the inverse problem, it is not necessary to confirm it experimentally with the results of physical measurements. The validity of its solution can be established by conducting numerical experiments on test problems synthesised using solutions to a previously verified direct problem, which is currently the case. Moreover, the synthesised variants of testing problems should be unique and not used at the previous stages of solving the inverse problem.

3. NUMERICAL MODELLING

According to the proposed methodology, one of its stages involves the creation of a computer homogeneous DOE on quasi-Sobol's sequences, which has low discrepancy rates both for the volumetric case and for two-dimensional projections.

In this research, the task of reconstructing the profiles of the EC and MP is carried out using a meta-model taking into account four factors σ, μ, and *f, z*, so then a combination of LP_τ-sequences ξ_1, ξ_6, ξ_{14}, ξ_{17} is used to implement a multidimensional homogeneous quasi-plan.

Figure 1 shows this type of DOE with improved two-dimensional projections on a unit scale, the numerical values of the point coordinates of which are given in Table 1.

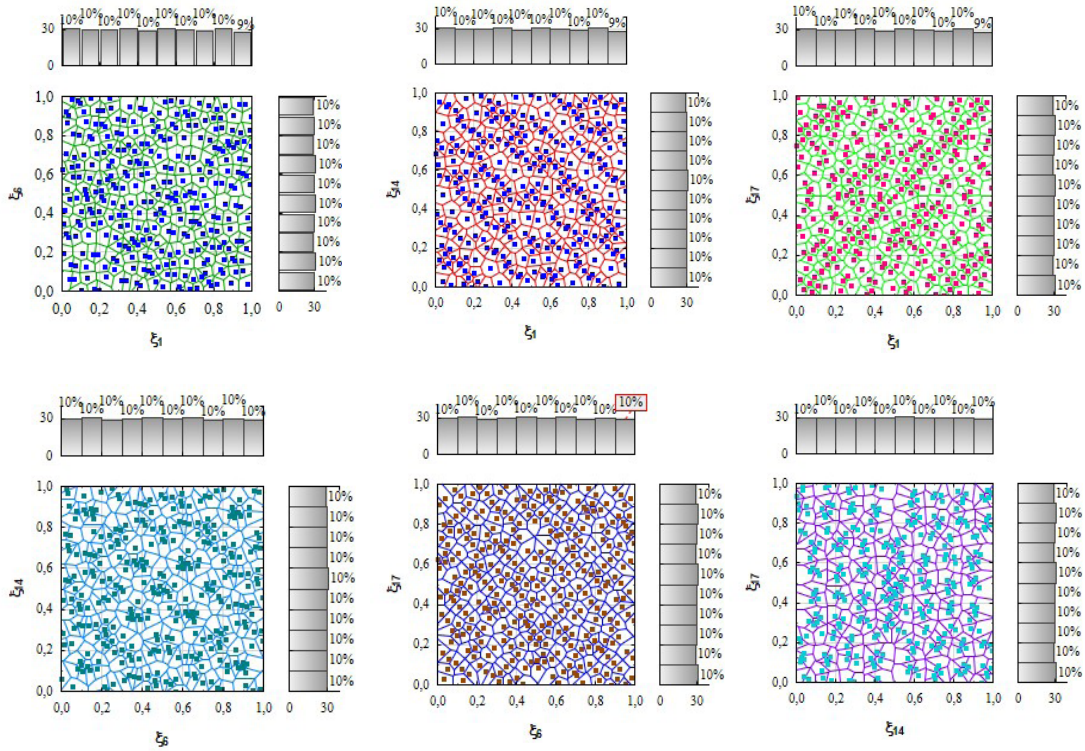

Fig. 1. Visualization of the projections of the experiment design on the LP_τ-sequences ξ_1, ξ_6, ξ_{14}, ξ_{17}.

The total number of DOE points is equal to $N_{profile}$ = 8191, but for the convenience of visualising the DOE homogeneity, only a limited number of them, namely 256, are shown in the figure. A visual analysis of the quality of DOE's 2D-projections using

Voronoi diagrams allows us to assess the degree of their homogeneity by the area of all formed segments. In addition, the homogeneity of the location of points in 2D-projections, even for such a small number of them, is also proved by the coordinate histograms of their distribution. With the number of $N_{profile}$ points, the situation with filling the projection space is even better.

Scaling helps make the transition from a single hyperspace to a real factor space. Initially, before the microstructure changes in the sub-surface zone, the MRO is characterised by the values of the EC σ_{deep} and MP μ_{deep}. When the MRO is exposed to any of the physical factors (temperature, deformation, etc.), the values of the EC and MP change to the maximum on their surface, remaining unchanged at a certain depth of the sub-surface zone. The reconstruction of profiles is performed within some a priori defined limits of their changes relative to the original ones. We will assume that the limits were set within ± 15 % relative to the initial values of the EC and MP on the surface of the MRO. If necessary, these limits can be adjusted.

Table 1 shows the numerical values of the electrophysical parameters μ_{surf} and σ_{surf} on the surface of the MRO at the DOE points in the real four-factor hyperspace. At the same time, point 1, which belongs to the primary profile, is characterised by the values of the EC $\sigma_{deep} = 2 \cdot 10^6$ S/m, $\sigma_{surf} = 9.2 \cdot 10^6$ S/m, and for the MC - $\mu_{deep} = 10$, $\mu_{surf} = 29.78$. Then, taking into account these limits, the ranges of change in the EC parameters on the surface of the MRO will be $7.82 \cdot 10^6 \leq \sigma_{surf} \leq 10.1 \cdot 10^6$ S/m; and for the MP – $24.531 \leq \mu_{surf} \leq 35.028$, with σ_{deep} and μ_{deep} being unchanged for any profile at the depth of the sub-surface zone.

In addition to the values of the electrophysical parameters, the creation of the DOE requires knowledge of the range of changes in the frequency of the electromagnetic excitation field $1 \leq f \leq 20$ kHz, which is informative for observing the signal response at different depths of its penetration, and the lift-off between the ECP and the surface of the MRO, which is taken to be $0.5 \leq z \leq 2.5$ mm.

Table 1. Experimental Design in Four-Factor Space

No point	Design in unit hyperspace				Design in real hyperspace			
	ξ_1	ξ_6	ξ_{14}	ξ_{17}	$\sigma_{surf} \cdot 10^6$, S/m	μ_{surf}	f, kHz	z, m
1	0.5	0.5	0.5	0.5	9.2	29.78	10.5	0.0015
2	0.25	0.75	0.75	0.25	9.89	27.155	15.25	0.001
3	0.75	0.25	0.25	0.75	8.51	32.405	5.75	0.002
4	0.125	0.125	0.125	0.875	8.165	25.8425	3.375	0.00225
5	0.625	0.625	0.625	0.375	9.545	31.0925	12.875	0.00125
…					…	…	…	
8188	0.249878	0.379761	0.497925	0.134644	8.868	27.1539	10.460	0.000769
8189	0.749878	0.879761	0.997925	0.634644	10.248	32.4039	19.960	0.001769
8190	0.499878	0.629761	0.747925	0.384644	9.558	29.7789	15.210	0.001269
8191	0.999878	0.129761	0.247925	0.884644	8.178	35.0289	5.710	0.002269

The laws of distribution of the EC "exponential" and the MP "Gaussian", referring to the typical dependencies determined experimentally in [11], [30] were used as an example, for the model piecewise stable representation of profiles.

Within the specified boundary limits of changes in electrophysical parameters in the

real design space (Table 1), we calculated the EC and MP distributions for all DOE points, which corresponds to the number of profiles in the total sample $N_{profile}$ with a sampling of the sub-surface zone $D = 3 \cdot 10^{-4}$ m by $L = 60$ conditional layers. For the sake of clarity, only some of the obtained profiles are shown in Fig. 2, along with a table that indicates their characteristic parameters.

For these variants of profiles and taking into account the frequency at which measurements are made and the values of the lift-off between the ECP and the MRO, the output signals of the ECP were calculated using the electrodynamic model (2), which are given in Table 2.

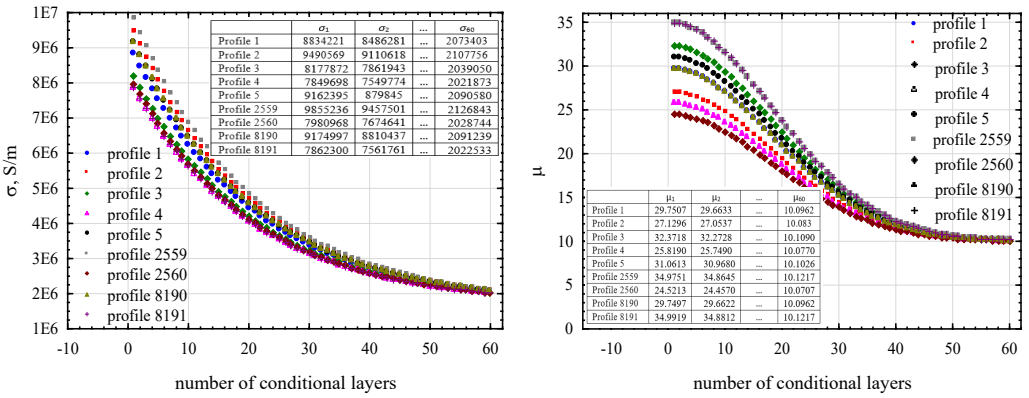

Fig. 2. MP and EC profiles in the sub-surface zone of the MRO for some of their cases.

Table 2. Training Set 8191×122 for Creating a Meta-model in the Full Factor Space

No profile	Re(e_{mod})	Im(e_{mod})	f, Hz	z, m
1	-2.618	-4.049	10500	0.0015
2	-3.344	-4.34	15250	0.001
3	-1.651	-3.074	5750	0.002
4	-1.082	-2.156	3375	0.00225
5	-3.021	-4.392	12875	0.00125
…				
8188	-2.721	-3.575	10460.1	0.0007692
8189	-3.82	-6.145	19960.1	0.0017692
8190	-3.338	-4.77	15210.1	0.0012692
8191	-1.602	-3.195	5710.1	0.0022692

In this case, the dimension of the factor space is 122, which is significant. Therefore, building a meta-model in such a space is not effective.

Therefore, the next stage of research is the transition to the reduced dimensionality space using the PCA method based on the SVD-decomposition of the Gram matrix created in the previous stage using the training set. The analysis of the obtained singular numbers allowed us to select 63 most influential eigenvectors for which the eigenvalues are greater than 1. Thus, to train the DFCNN, we use a matrix of parameters in a low-dimensional factor space of size $N_{profile} \times n_{red}$, where $n_{red} = 63$ is the number of basis vectors **g** in the new space (Table 3). The total number of samples in the selec-

tion was distributed in the following ratio: N_{traine} = 4209 for training, $N_{NN\text{-}test}$ = 904 for testing, and N_{CV} = 904 for cross-validation. The remaining 2177 samples were not used in training, but some of them were later used as synthesised data to check the reliability of the solution to the inverse profile reconstruction problem.

Table 3. Training Set of 8191×63 for Creating a Meta-model in Low-dimensional Factor Space

No point	g_1	g_2	…	g_{62}	g_{63}
1	-34344006	-40876.45	…	-0.2349043	0.0011182417
2	-36406779	469672.51	…	0.4565146	0.0013578367
3	-32281232	-551426.58	…	0.2288428	-0.00084519701
4	-31249845	-806701.24	…	0.2274442	0.00081916363
5	-35375392	214397.8	…	0.2335731	-0.00072947157
…	…	…	…		
8188	-33352224	-286351.94	…	0.6077515	-0.00050085944
8189	-37477772	734747.26	…	0.2040051	0.00094150458
8190	-35414998	224197.78	…	0.0311096	-0.0005216811
8191	-31289451	-796901.49	…	-0.1805091	-0.00094330238

As mentioned in the previous section, further construction of meta-models is carried out by means of deep learning neural networks, for which the outputs of each of the two networks are, respectively, the real and imaginary parts of the ECP EMF, and the inputs are the matrix of **g**-parameters. As a result, we obtained the deep networks Re-MLP-16-17-15-11-1 and Im-MLP-16-17-16-11-1 with four hidden layers for the real and imaginary parts of the EMF, respectively. The validity of the obtained meta-models was assessed by: histograms of residuals (Figs. 3 a, 4 a); Normal P-Plot of residuals (Figs. 3 b, 4 b); scatter plots (Figs. 3 c, 4 c) and $MAPE_{metamod}$ errors, % (Mean Absolute Percentage Error) separately for training, cross-validation and test samples; Box-plots (Figs. 3 d, 4 d).

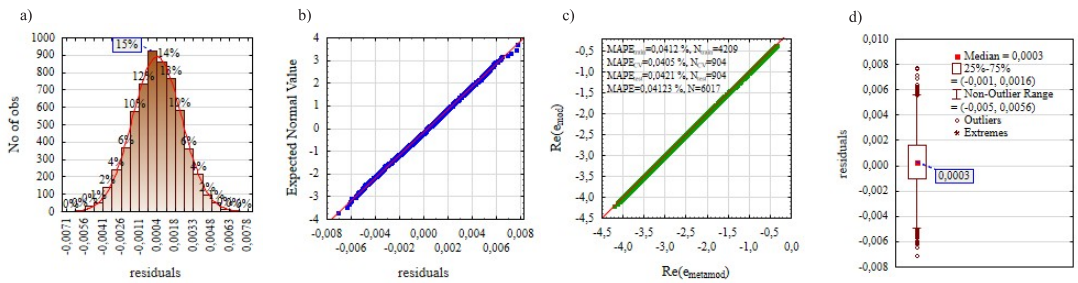

Fig. 3. Statistical assessment of the quality of the Re-MLP-16-17-15-11-1 meta-model:
a – histogram of the residuals distribution; b – Normal P-Plot of the residuals;
c – scatter plot; d – box plot.

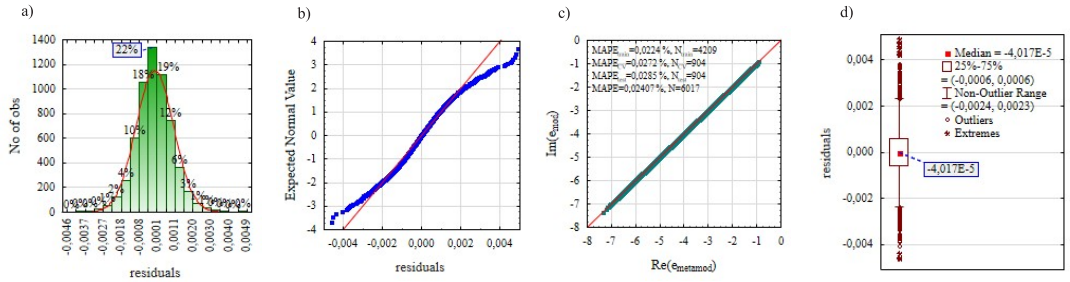

Fig. 4. Statistical assessment of the quality of the meta-model Im-MLP-16-17-16-11-1: a – histogram of the residuals distribution; b – Normal P-Plot; c – scatter plot; d – box plot.

A preliminary assessment of the adequacy of the created meta-models was performed by testing the hypothesis of the normality of the distribution of residuals according to the criteria of skewness and kurtosis with an assessment of the reliability of the obtained coefficients by Student's t-test.

In addition, according to the numerical indicators of the coefficient of determination and Fisher's *F*-ratio $F^{total}_{\nu_D;\nu_R} = MS_D / MS_R$, where MS_D is the mean square of the regression, MS_R is the mean square of the residuals (ν_D = 63, ν_R = 6017-63-1 = 5953), the informativeness and adequacy of the created meta-models (Table 4) were tested at the level of significance of 5 %.

Both of the created meta-models are adequate, since the calculated model values of the Fisher's criterion for them significantly exceed its critical value. The high informativeness of the created meta-models is also indicated by a significant coefficient of determination, which is significantly reliable according to Fisher's criterion at the level of 5 %.

Table 4. The Verification of the Adequacy and Informativeness of Meta-models

Parameters	Meta-models	
	Re-MLP-16-17-15-11-1	Im-MLP-16-17-16-11-1
Adequacy with ν_D = 63, ν_R = 5953, α = 5 %	$F^{total}_{63;5953} = 7.279 \cdot 10^8$ $F^{table}_{0.05;63;5953} = 1.312$	$F^{total}_{63;5953} = 1.789 \cdot 10^8$ $F^{table}_{0.05;63;5953} = 1.312$
Informativeness	$R^2 = 0.9999$; $F^{total}_{63;5953} = 7.285 \cdot 10^7$	$R^2 = 0.999999$; $F^{total}_{63;5953} = 1.7893 \cdot 10^8$

The inverse problem was solved using a metaheuristic stochastic global optimisation algorithm, namely, a hybrid multiagent particle swarm optimisation algorithm with evolutionary formation of the swarm composition, the effectiveness of which has been proven in [31], [32]. To raise the accuracy of solutions, the multi-start technique was used in the research. Thirty-nine solutions were obtained by a series of starts of the optimisation algorithm, and inverse transformations were performed from the PCA space of the principal components to the primary space and the actual MP and EC profiles were obtained for four test measurements of the EMF.

The bounds within which the MAPE errors of the profiles in thirty-nine starts are obtained are given in Table 5, and Fig. 5 shows the percentage distribution of these errors in the range from minimum to maximum for one *Test 1* measurement as an example.

The reconstructed EC and MP profiles

are finally obtained by averaging the profile variants for each test measurement. Table 6 shows the values of the original and reconstructed profiles and the MAPE, % error, for four test measurements.

Table 5. Ranges of Change in MAPE Error of Reconstruction of Profile Variants

Parameters		Measurements			
		Test 1	*Test 2*	*Test 3*	*Test 4*
Re(e_{mes})		-0.58	-1.094	-1.609	-2.557
Im(e_{mes})		-1.236	-2.045	-2.641	-3.827
f, Hz		1533.52	3205.9	5098.3	9599.4
z, mm		1.065	1.086	1.0446	1.0068
$MAPE_{\mu}$, %	min	0.154	0.324	0.138	0.235
	max	9.255	8.483	8.874	6.75
$MAPE_{\sigma}$, %	min	0.248	0.17	0.198	0.322
	max	4.258	4.824	5.62	3.854

Table 6. Reconstructed MP and EC Profiles Based on the Results of Averaging

Parameters		Conditional layers				
		1	2	…	59	60
Test 1	μ_{test1}	30.31168	30.22174		10.11804	10.09899
	μ_{recon1}	30.23665	30.14696		10.10688	10.08789
	$MAPE_{\mu}$,%	0.178				
	$\sigma_{test1}\times10^6$, S/m	8.277112	7.956343		2.061894	2.044244
	$\sigma_{recon1}\times10^6$, S/m	8.254753	7.934985		2.058932	2.041337
	$MAPE_{\sigma}$,%	0.204				
Test 2	μ_{test2}	34.63338	34.52431		10.14316	10.12005
	μ_{recon2}	34.76038	34.65093		10.18557	10.16238
	$MAPE_{\mu}$,%	0.391				
	$\sigma_{test2}\times10^6$, S/m	7.782724	7.486066		2.034691	2.018368
	$\sigma_{recon2}\times10^6$, S/m	7.759168	7.464006		2.040130	2.023889
	$MAPE_{\sigma}$,%	0.157				
Test 3	μ_{test3}	30.96801	30.87516		10.12185	10.10219
	μ_{recon3}	30.89312	30.80050		10.0945	10.07488
	$MAPE_{\mu}$,%	0.256				
	$\sigma_{test3}\times10^6$, S/m	7.890392	7.588483		2.040615	2.024003
	$\sigma_{recon3}\times10^6$, S/m	7.858705	7.558117		2.034522	2.017983
	$MAPE_{\sigma}$,%	0.347				
Test 4	μ_{test4}	30.9439	30.85115		10.12171	10.10207
	μ_{recon4}	30.80823	30.71591		10.083898	10.064342
	$MAPE_{\mu}$,%	0.405				
	$\sigma_{test4}\times10^6$, S/m	7.574084	7.287602		2.023211	2.007448
	$\sigma_{recon4}\times10^6$, S/m	7.564644	7.278311		2.016711	2.000954
	$MAPE_{\sigma}$,%	0.228				

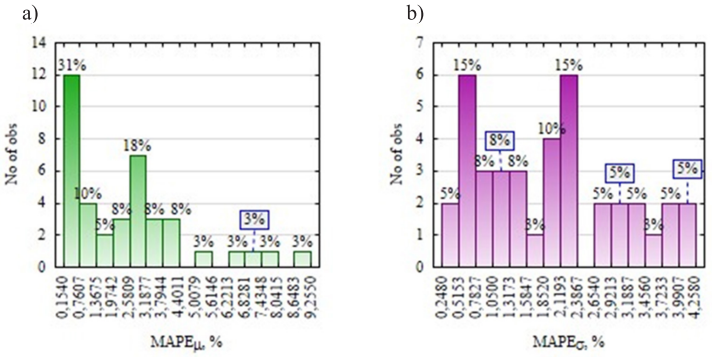

Fig. 5. MAPE error distribution diagrams of reconstructed profile variants for *Test 1* measurement: a – for magnetic permeability; b – for electrical conductivity.

4. DISCUSSION AND CONCLUSION

Studies similar in methodology were performed with a limited number of influential factors in the meta-models taken into account a priori. Thus, in the first case, only two factors were taken into account, namely μ and σ; and in the second case, three factors μ, σ, *f* were taken into account, i.e., the multi-frequency mode of ECP operation was considered. In all cases, numerical experiments were performed according to an identical scheme.

The MAPE error of the results of profile identification taking into account only two factors in the active compact space was 0.352 % for the MP profiles and 0.96 % for the EC profiles. When more factors μ, σ, *f* are taken into account in the meta-model, the following results of profile identification are obtained for the best case: for MP – 0.275 % and for EC – 0.354 %. A decrease in profile reconstruction errors was observed compared to studies where only two factors were taken into account in the meta-models. Model calculations of the reconstruction of the electrophysical parameters of planar MRO's in the presence of a priori information on μ, σ, *f*, *z* based on the results of direct measurements of the EMF amplitude and phase, which are presented in Table 6, give, in the best case, the MAPE errors for the MP profile – 0.178 %, and for the EC – 0.157 %.

A comparative analysis of the accuracy of the above numerical modelling experiments shows that there is a tendency to improve the results of determining the profiles with an increase in the amount of a priori information about the MRO contained in the meta-models. The best results are demonstrated when the meta-model contains complete information on the most influential factors. It is interesting to note that even with some loss of information caused by the reduction of the design space during optimization, the previously mentioned trend is observed. It is also important to be able to control information losses when reducing the space by making compromise decisions regarding the balance between the size of the space and the accuracy of the problem, which becomes an additional effective means of performing modelling studies to improve the results.

Thus, the studies have convincingly demonstrated the advantages of the proposed method for reconstructing the electrophysical parameter profiles of planar MRO's based on the results of one-time

measurements by eddy current probes using surrogate optimisation techniques and accumulating the full volume of the most important a priori information on the modes of electromagnetic research of objects.

REFERENCES

1. Hampton, J., Fletcher, A., Tesfalem, H., Peyton, A., & Brown, M. (2022). A Comparison of Non-linear Optimisation Algorithms for Recovering the Conductivity Depth Profile of an Electrically Conductive Block Using Eddy Current Inspection. *NDT & E International*, *125*, 102571.
2. Cui, Z., Wang, Q., Xue, Q., Fan, W., Zhang, L., Cao, Z., ... & Yang, W. (2016). A Review on Image Reconstruction Algorithms for Electrical Capacitance/Resistance Tomography. *Sensor Review*, *36* (4), 429–445.
3. Xia, Z., Huang, R., Chen, Z., Yu, K., Zhang, Z., Salas-Avila, J. R., & Yin, W. (2022). Eddy Current Measurement for Planar Structures. *Sensors*, *22* (22), 8695.
4. Tesfalem, H., Hampton, J., Fletcher, A. D., Brown, M., & Peyton, A. J. (2021). Electrical Resistivity Reconstruction of Graphite Moderator Bricks from Multi-Frequency Measurements and Artificial Neural Networks. *IEEE Sensors Journal*, *21* (15), 17005–17016.
5. Lu, M. (2018). *Forward and Inverse Analysis for Non-destructive Testing Based on Electromagnetic Computation Methods*. The University of Manchester (United Kingdom).
6. Liu, G. R., & Han, X. (2003). *Computational Inverse Techniques in Nondestructive Evaluation*. CRC press.
7. Jiang, P., Zhou, Q., Shao, X., Jiang, P., Zhou, Q., & Shao, X. (2020). *Surrogate-Model-Based Design and Optimization* (pp. 135–236). Springer Singapore.
8. Zhang, J., Yuan, M., Xu, Z., Kim, H. J., & Song, S. J. (2015). Analytical Approaches to Eddy Current Nondestructive Evaluation for Stratified Conductive Structures. *Journal of Mechanical Science and Technology*, *29*, 4159–4165.
9. Lei, Y. Z. (2018). General Series Expression of Eddy-Current Impedance for Coil Placed above Multi-Layer Plate Conductor. *Chinese Physics B*, *27* (6), 060308.
10. Bowler, N. (2019). *Eddy-Current Nondestructive Evaluation*. New York: Springer.
11. Uzal, E. (1992). *Theory of Eddy Current Inspection of Layered Metals*. Iowa State University.
12. Theodoulidis, T. P., & Kriezis, E. E. (2006). Eddy Current Canonical Problems (with Applications to Nondestructive Evaluation). 107503116
13. Trembovetska, R., Halchenko, V., & Bazilo, C. (2022, June). Inverse multi-parameter identification of plane objects electrophysical parameters profiles by eddy-current method. In *International Conference on Smart Technologies in Urban Engineering* (pp. 202–212). Cham: Springer International Publishing.
14. Halchenko, V., Trembovetska, R., Bazilo, C., & Tychkova, N. (2022, June). Computer simulation of the process of profiles measuring of objects electrophysical parameters by surface eddy current probes. In *International Scientific-Practical Conference "Information Technology for Education, Science and Technics"* (pp. 411–424). Cham: Springer Nature Switzerland.
15. Dodd, C. V., & Deeds, W. E. (1975). *Calculation of Magnetic Fields from Time-Varying Currents in the Presence of Conductors* (No. ORNL-TM-4958). Oak Ridge National Lab. (ORNL), Oak Ridge, TN (United States).
16. Philippe, A. (1969). *Contrôle non destructif par courants de Foucault*. Contribution à l'étude de l'influence de la forme des sondes bobinées sur la distribution spatiale de'induction magnétique. EUR 4284.

17. Kawashima, K. (1975). *Electromagnetic Ultrasonic Transducer* (No. ORNL-5063). Oak Ridge National Lab (ORNL), Oak Ridge, TN (United States).
18. Halchenko, V., Trembovetska, R., Tychkov, V., & Tychkova, N. (2023). Construction of Quasi-DOE on Sobol's Sequences with Better Uniformity 2D Projections. *Applied Computer Systems*, *28* (1), 21–34.
19. Wang, Y., Sun, F., & Xu, H. (2022). On Design Orthogonality, Maximin Distance, and Projection Uniformity for Computer Experiments. *Journal of the American Statistical Association*, *117* (537), 375–385.
20. Fang, K., Liu, M. Q., Qin, H., & Zhou, Y. D. (2018). *Theory and Application of Uniform Experimental Designs* (Vol. 221). Singapore: Springer.
21. Ping, H., Lin, D. K., Min-Qian, L., Qingsong, X., & Yongdao, Z. (2020). Theory and Application of Uniform Designs. *Scientia Sinica Mathematica*, *50* (5).
22. Halchenko, V. Y., Yakimov, A. N., & Ostapuschenko, D. L. (2010). Global Optimum Search of Functions with Using of Multiagent Swarm Optimization Hybrid with Evolutional Composition Formation of Population. *Information Technology*, *10*, 9–16.
23. Halchenko, V. Y., Trembovetska, R. V., Tychkov, V. V., & Storchak, A. V. (2019). Nonlinear Surrogate Synthesis of the Surface Circular Eddy Current Probes. *Przegląd elektrotechniczny*, *9*, 76–82.
24. Kuznetsov, B., Bovdui, I., & Nikitina, T. (2021, February). Optimal design of system of active shielding of magnetic field generated by overhead power lines. In *2021 IEEE 16th International Conference on the Experience of Designing and Application of CAD Systems (CADSM)* (pp. 1–4). IEEE.
25. Koshevoy, N. D., & Beliaieva, A. A. (2017). Application of Particle Swarm Optimization of Composite Second Order Plans. *Radioelectronic and Computer Systems*, *1*, 69–75.
26. Géron, A. (2022). *Hands-on Machine Learning with Scikit-Learn, Keras, and TensorFlow*. O'Reilly Media, Inc.
27. Wang, J., Zhou, J., & Chen, X. (2022). *Data-Driven Fault Detection and Reasoning for Industrial Monitoring*. Springer Nature.
28. Géron, A. (2017). *Deep Learning avec TensorFlow*. Dunod.
29. Raschka, S. (2017). *Machine Learning*. Packt.
30. Galchenko, V. Y., Koshevoy, N. D., & Trembovetskaya, R. V. (2022). Homogeneous Plans of Multi-Factory Experiments on Quasi-Random R-Roberts Sequences for Surrogate Modeling in a Vortex Style Structuroscopy. *Radio Electronics, Computer Science, Control*, *62* (3), 22–30.
31. Halchenko, V. Y., Trembovetska, R., & Tychkov, V. (2021). Surrogate Synthesis of Frame Eddy Current Probes with Uniform Sensitivity in the Testing Zone. *Metrology and Measurement Systems*, *28* (3).
32. Halchenko, V. Y., Trembovetska, R. V., & Tychkov, V. V. (2021). Surrogate Synthesis of Excitation Systems for Frame Tangential Eddy Current Probes. *Archives of Electrical Engineering*, *70* (4), 743–757.